

## Ultrasonic velocities in amorphous $\text{As}_2\text{S}_3$ and $\text{As}_2\text{Se}_3$ between 1.5 and 296 K

T. N. Claytor\* and R. J. Sladek

*Department of Physics, Purdue University, West Lafayette, Indiana 47907*

(Received 30 June 1978)

The velocities of ultrasonic longitudinal and transverse (shear) waves have been measured in amorphous  $\text{As}_2\text{S}_3$  and  $\text{As}_2\text{Se}_3$  between 1.5 K and room temperature. No dependence of frequency was found in the 10- to 90-MHz range employed. The velocities increased monotonically with decreasing  $T$ . The increase down to about 40 K is interpreted as being due to the anharmonicity of atomic vibrations. Using simplified versions of expressions developed by others for crystalline solids, we deduce ( $T$ -dependent) ultrasonic  $\gamma$ 's from our longitudinal-wave data, which allow successful calculation of shear-wave velocities versus temperature down to 40 K. The ultrasonic  $\gamma$ 's are consistent with Grüneisen, elastic, and Raman-mode  $\gamma$ 's. At lower  $T$  the velocities are more temperature dependent than implied by the quasi-harmonic model. We interpret them in terms of relaxation processes involving thermal phonon-assisted tunneling in two-level systems. Curves calculated from theoretical expressions from the literature are fitted to our data below 7 K, yielding information about the distribution of two-level systems and values for deformation potentials.

### I. INTRODUCTION

The velocity and attenuation of ultrasonic waves in glasses have been subjected to intensive investigation in recent years.<sup>1-4</sup> Motivation for such work was provided by the development of the double-potential-well (DPW) model<sup>5,6</sup> for explaining heat-capacity and thermal-transport data in glasses at very low temperatures.<sup>7,8</sup> The DPW model also made a prediction about resonant ultrasonic absorption<sup>5</sup> due to tunneling of atoms between potential wells, and has been extended<sup>1</sup> to describe the concomitant effect on the velocity.<sup>9</sup> Theory has also been developed for how relaxation processes involving thermal-phonon-assisted tunneling between wells affect both the attenuation<sup>10</sup> and velocity<sup>9</sup> of ultrasonic waves.

Between liquid-helium and room temperatures, tetrahedrally bonded glasses have been found<sup>11,12</sup> to exhibit a velocity minimum whose temperature depends on the particular glass in question. Hopping of atoms over the potential barrier between wells and structural effects have been invoked to explain the ultrasonic attenuation<sup>13,14</sup> observed in this range for tetrahedral glasses.

In view of the interesting behavior of ultrasound in tetrahedrally bonded glasses and of the ultrasonic attenuation in glasses comprised of  $\text{As}_2\text{S}_3$  (Ref. 2) or  $\text{As}_2\text{Se}_3$  (Refs. 3, 4) (also referred to herein as amorphous, and hence as  $\alpha$ - $\text{As}_2\text{S}_3$  and  $\alpha$ - $\text{As}_2\text{Se}_3$ ), we decided to investigate ultrasonic velocities in these materials, which are pyramidally bonded.

It will be seen that in contrast to the tetrahedrally bonded glasses,  $\alpha$ - $\text{As}_2\text{S}_3$  and  $\alpha$ - $\text{As}_2\text{Se}_3$  have velocities which increase monotonically with decreasing temperature between room temperature

and 1.5 K. The behavior down to 40 K is found to be describable by means of a quasi-harmonic (QH) Debye model like that used for crystalline solids, and from it we deduce a  $T$ -dependent ultrasonic  $\gamma$  for each glass. At lower temperatures the velocities have more  $T$  dependence than implied by the QH model. This can be attributed to relaxation processes involving thermal-phonon-assisted tunneling in two-level systems.<sup>1</sup> Theoretical expressions will be fitted to our data at lowest temperatures, yielding a distribution (in energy) of the two-level systems and values for deformation potentials.

### II. EXPERIMENTAL DETAILS

#### A. Method and apparatus

We used the pulse-echo overlap method<sup>15</sup> with commercial electronic instrumentation. The transducers, bonding, and thermal environment employed followed those described in Ref. 2.

The velocity was determined from the frequency needed to overlap selected echoes (and the path length deduced from the sample size). In order to increase sensitivity at the lowest temperature, we often overlapped echoes 2 and 18, giving a velocity resolution of approximately  $5 \times 10^{-6}$  at a frequency of 30 MHz. At higher temperatures ( $T > 70$  K), where the resolution did not have to be as great, we often used echoes 2 and 6.

#### B. Samples

Optical quality  $\alpha$ - $\text{As}_2\text{Se}_3$  was kindly furnished by Kariya of the Nikon Co., and the  $\alpha$ - $\text{As}_2\text{S}_3$  was purchased from the American Optical Co. Raman

TABLE I. Impurity concentration ratios obtained from a commercial mass-spectrographic analysis of our sample material.

Material	Impurity element <sup>a</sup>	$N_I/(N_{\text{As}} + N_{\text{C}})$ <sup>b</sup> (ppm)
$\alpha\text{-As}_2\text{S}_3$	Sb	200
	Cl	14
	K	13
	Fe	9
	Ca	6
$\alpha\text{-As}_2\text{Se}_3$	Sb	1000
	Bi	500
	Pb	50
	Fe	30
	Cl	5
	Na	5

<sup>a</sup> Elements not listed are either below the detection limit, or equal to or less than 2 ppm.

<sup>b</sup>  $N_I$ ,  $N_{\text{As}}$ , and  $N_{\text{C}}$  are the number of impurity, As, and S or Se atoms, respectively.

measurements, kindly performed on  $\alpha\text{-As}_2\text{S}_3$  by Galeener and Mosby of the Xerox Palo Alto Research Center, and on  $\alpha\text{-As}_2\text{Se}_3$  by Nemanich of the University of Chicago, failed to detect appreciable departures from stoichiometry. Infrared transmission measurements on  $\alpha\text{-As}_2\text{S}_3$  revealed the presence of a small, insignificant amount of oxygen. Major chemical impurities obtainable from a mass-spectrographic analysis (by Battelle Memorial Institute) are listed in Table I. Densities were measured to be  $3.210 \text{ gm/cm}^3$  for  $\alpha\text{-As}_2\text{S}_3$  and  $4.635 \text{ g/cm}^3$  for  $\alpha\text{-As}_2\text{Se}_3$  at  $23^\circ\text{C}$  using the Archimedes method with water and a sensitive microbalance.

Our samples were lapped flat to 2–3 fringes of sodium light over a  $1\text{-cm}^2$  area with the flats being parallel to  $20''\text{--}30''$ . Successively finer powders were used ending with  $0.5\text{-}\mu\text{m Al}_2\text{O}_3$ . The  $\alpha\text{-As}_2\text{S}_3$  material was checked optically for cracks and bubbles under a microscope, and also was inspected under crossed polaroids for strains. Only very diffuse strains were found in the experimental volume of the sample, and seemed to be about the same size as those caused by mounting the sample in its holder or by holding the sample with tweezers. Since they are opaque, the  $\alpha\text{-As}_2\text{Se}_3$  samples were subjected to an inspection with an infrared microscope. The  $\alpha\text{-As}_2\text{Se}_3$  sample selected for measurement was clear and free of cracks and bubbles. Samples of  $\alpha\text{-As}_2\text{Se}_3$  were about  $1.0 \times 1.0 \times 0.5 \text{ cm}^3$  in size and samples of  $\alpha\text{-As}_2\text{S}_3$  were about  $1.9 \times 1.9 \times 0.7 \text{ cm}^3$ , with the length in the direction of propagation being measured accurately with an electronic gauge.

Below room temperature sample length was corrected for thermal contraction using expansivity data obtained using a Theta Industries silica pushrod LVDT dilatometer (mounted in a Cryogenics Associates Dewar). Although our  $\Delta L/L$  data<sup>3</sup> extended only down to 20 K, we did use them to estimate sample lengths down to 1.5 K. Such extrapolation was justified because  $\Delta L/L$  is almost independent of  $T$  at the lowest temperatures we reached, and because it yielded values in agreement with recent expansivity measurements down to 4.2 K by others.<sup>16</sup>

### C. Dispersion check, overlap criteria, and errors

An investigation of the frequency dependence of the velocity at 295 K was undertaken because it has been reported<sup>2</sup> that the velocity was dispersive in  $\alpha\text{-As}_2\text{S}_3$ . We found no measurable dispersion (i.e., less than 0.3%) between 10 and 50 MHz in either  $\alpha\text{-As}_2\text{S}_3$  or  $\alpha\text{-As}_2\text{Se}_3$  at room temperature. While looking for dispersion, we checked our echo-overlap technique by using different sample lengths and various radio frequencies to remove any ambiguity that might arise from improper overlapping of echoes. The reproducibility of our bonds was found to yield a precision of about  $\pm 0.05\%$  in the velocity. The absolute accuracy was probably lower, on the order of 0.2%–0.4%, because of phase shifts caused by the transducer and the bond. Different samples of  $\alpha\text{-As}_2\text{Se}_3$  had longitudinal-wave velocities differing by as much as 0.3% at 296 K.

## III. RESULTS

Figures 1–4 show our velocity data for 30-MHz ultrasound over our entire temperature range of

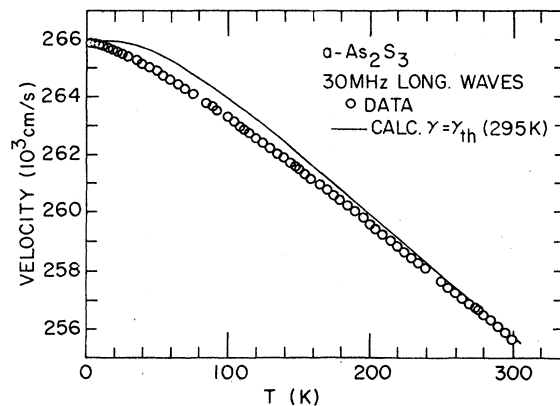


FIG. 1. Longitudinal-wave velocity data and curve calculated using Eq. (4) and the room-temperature thermodynamic Grüneisen  $\gamma$ .

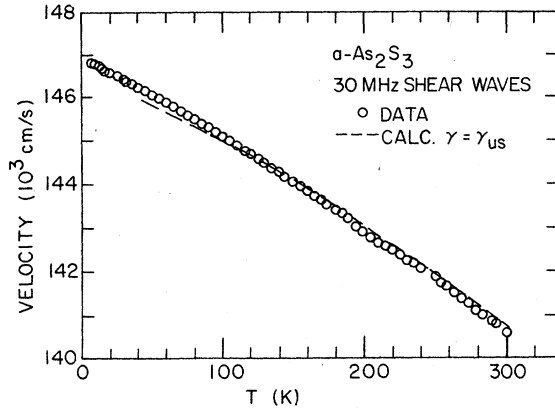


FIG. 2. Shear-wave velocity data and curve calculated as indicated in Sec. IV A using the ultrasonic  $\gamma$  deduced from fitting longitudinal velocity data.

1.5–296 K. Each velocity decreases monotonically with increasing temperature. Total changes between 1.5 and 296 K are about  $-4.1\%$  and  $-4.5\%$  for longitudinal and shear waves in  $\alpha$ - $\text{As}_2\text{S}_3$ , and short  $-4.1\%$  and  $-4.4\%$  for the respective waves in  $\alpha$ - $\text{As}_2\text{Se}_3$ .

Our low-temperature data are shown in detail in Figs. 5–8 as plots of  $-\Delta v/v$ , where  $\Delta v = v(T) - v(1.5 \text{ K})$ , for 30-MHz longitudinal and shear waves, and for 10- or 90-MHz longitudinal waves. There is no significant dependence of  $-\Delta v/v$  on frequency (see Figs. 5 and 7). In both  $\alpha$ - $\text{As}_2\text{S}_3$  and  $\alpha$ - $\text{As}_2\text{Se}_3$ , corresponding waves have very similar values of  $-\Delta v/v$ . For each material,  $-\Delta v/v$  is greater for shear waves than for longitudinal waves.

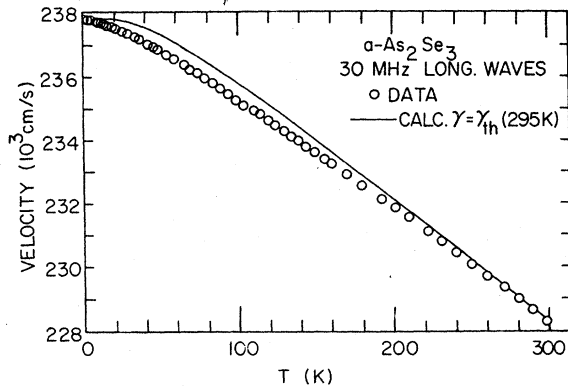


FIG. 3. Longitudinal-wave velocity data and curve calculated using Eq. (4) and the room-temperature thermodynamic Grüneisen  $\gamma$ .

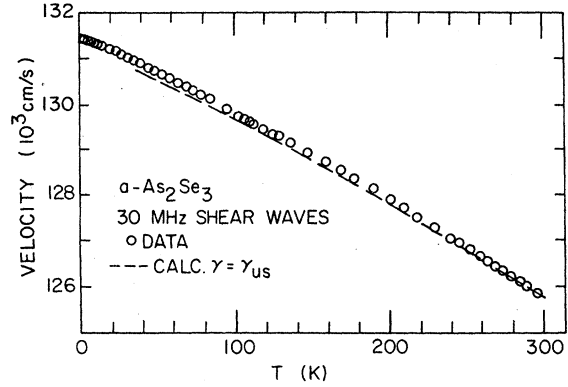


FIG. 4. Shear-wave velocity data and curve calculated as indicated in Sec. IV A using the ultrasonic  $\gamma$  deduced from fitting longitudinal velocity data.

## IV. DISCUSSION

### A. Quasiharmonic regime

From 296 to about 40 K, the temperature dependence of the velocities of both longitudinal and shear waves in  $\alpha$ - $\text{As}_2\text{S}_3$  and  $\alpha$ - $\text{As}_2\text{Se}_3$  can be understood in terms of a simplified version of the QH atomic oscillator model developed for crystalline solids in general by Leibfried and Ludwig<sup>17</sup> and for cubic crystals by Garber and Granato<sup>18</sup> (GG). By adapting the results of GG to the case of iso-

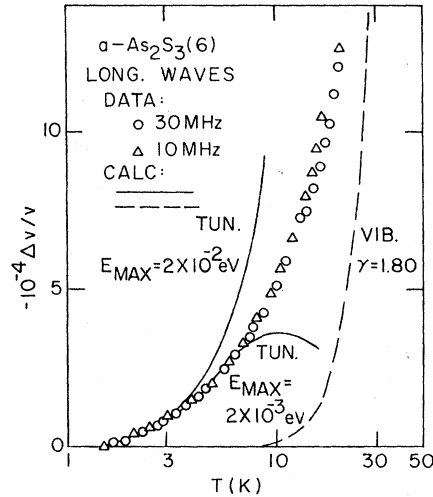


FIG. 5. Fractional change of longitudinal velocity measured and calculated at low temperatures. The solid curves for relaxation processes involving single-thermal-phonon-assisted tunneling between sites are calculated using Eqs. (8)–(10), and the dashed curve for vibrational anharmonicity is calculated using Eq. (1) and the low-temperature elastic  $\gamma$ . Using the Gaussian distribution given by Eq. (11), we obtained a curve identical to that marked TUN.  $E_{\text{max}} = 2 \times 10^{-3} \text{ eV}$ .

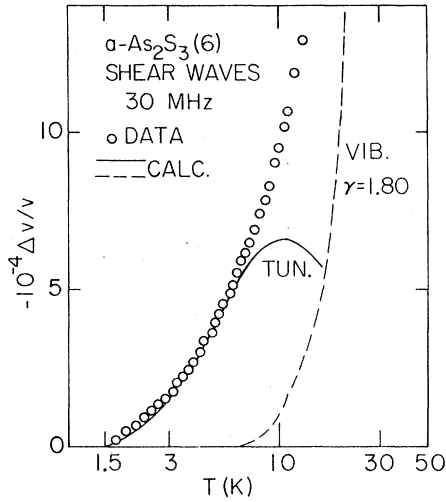


FIG. 6. Fractional change of shear velocity measured and calculated at low temperatures. The solid curve for relaxation via tunneling is calculated using Eqs. (8), (9), and (11), and the dashed curve for vibrational anharmonicity is calculated using Eq. (5) and the low-temperature elastic  $\gamma$ .

tropy and assuming that all vibrational modes have the same anharmonicity parameter,  $\gamma = -\partial \ln \omega / \partial u$ , with  $\omega$  the angular frequency of the mode and  $u$  the strain, we obtain for  $C_l$ , the adiabatic stiffness modulus of longitudinal waves,

$$C_l = C_l^0 + \frac{1}{V} \left\{ -\gamma^2 - \gamma \left[ \left( \frac{\partial C_l}{\partial P} \right)_T - \frac{C_l}{3B} \right] \right\} U, \quad (1)$$

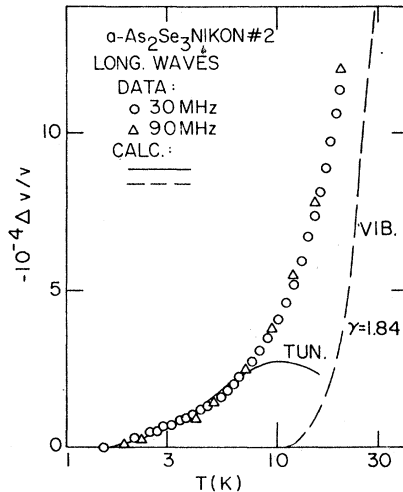


FIG. 7. Fractional change of longitudinal velocity measured and calculated at low temperatures. The solid curve for relaxation via tunneling is calculated using Eqs. (8), (9), and (11), and the dashed curve for vibrational anharmonicity is calculated using Eq. (1) and the low-temperature elastic  $\gamma$ .

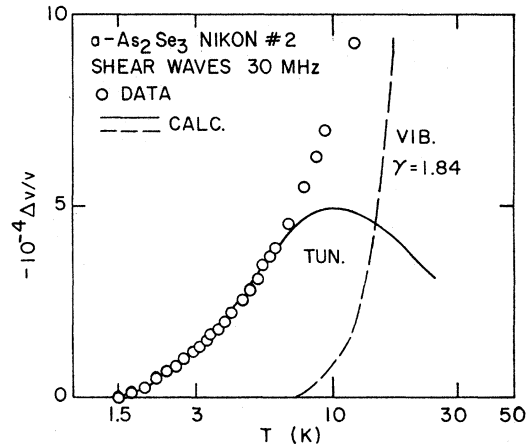


FIG. 8. Fractional change of shear velocity measured and calculated at low temperatures. The solid curve for relaxation via tunneling is calculated using Eqs. (8), (9), and (11), and the dashed curve for vibrational anharmonicity is calculated using Eq. (5) and the low-temperature elastic  $\gamma$ .

where  $C_l^0$  is the elastic stiffness at  $T=0$ ,  $V$  is the volume,  $(\partial C_l / \partial P)_T$  is the change of modulus with pressure at constant  $T$ ,  $B$  is the bulk modulus, and  $U$  is the total energy of the atomic oscillations. [In Eq. (1) the term containing  $-\gamma^2$  results from the  $\gamma^2 - \partial \gamma / \partial u$  term given by GG when  $\partial \gamma / \partial u$  is approximated by  $-2\gamma^2$ .] The quantity  $U$  in Eq. (1) is, according to the Debye model for solids,

$$U = 3Nk_B \Theta \left[ 3 \left( \frac{T}{\Theta} \right)^4 \int_0^{\Theta/T} \frac{x^3 dx}{e^x - 1} \right] = 3Nk_B \Theta F \left( \frac{T}{\Theta} \right), \quad (2)$$

where  $N$  is the number of atoms in volume  $V$ ,  $k_B$  is Boltzmann's constant,  $x = k_B T$ , and  $\Theta$  is the elastic Debye temperature obtained from the ultrasonic velocities measured at low temperatures using the relation

$$\Theta = \frac{h}{k_B} \left( \frac{3N}{4\pi V} \right)^{1/3} \left( \frac{1}{v_l^3} + \frac{2}{v_t^3} \right)^{-1/3}. \quad (3)$$

In Eq. (3)  $h$  is Planck's constant. Table II contains the values of  $\Theta$  for  $\alpha$ - $As_2S_3$  and  $\alpha$ - $As_2Se_3$ .

As a first check on the applicability of Eqs. (1) and (2), we use them to calculate  $\Delta C_l / C_l = [C_l(296 \text{ K}) - C_l(1.5 \text{ K})] / C_l$ , and compare the results with those obtained using measured changes in velocity  $v_l$  and sample length  $L$  between 1.5 and 296 K in the expression  $2\Delta v_l / v_l + 3\Delta L / L$ , since  $C_l = \rho v_l^2$  and  $\Delta L = L(T) - L(296 \text{ K})$ . In order to calculate  $\Delta C_l / C_l$ , we take  $\gamma$  to be equal to the thermodynamic Grüneisen  $\gamma_{th}$  at room tempera-

TABLE II. Values of various quantities used in calculating the changes in elastic moduli with temperature from Eqs. (1) and (5) of the text. Room-temperature values are given except in the case of  $\Theta$  which is for 1.5 K.

Quantity	Units	<i>a</i> -As <sub>2</sub> S <sub>3</sub>	<i>a</i> -As <sub>2</sub> Se <sub>3</sub>
$\Theta$	K	165	144
$C_l$	10 <sup>11</sup> dyn/cm <sup>2</sup>	2.10	2.415
$C_t$	10 <sup>11</sup> dyn/cm <sup>2</sup>	0.635	0.731
$B$	10 <sup>11</sup> dyn/cm <sup>2</sup>	1.25	1.44
$\left(\frac{\partial C_l}{\partial P}\right)_T$	...	9.3 <sup>a</sup>	8.8 <sup>a</sup>
$\left(\frac{\partial C_t}{\partial P}\right)_T$	...	1.9 <sup>a</sup>	1.9 <sup>a</sup>

<sup>a</sup> D. Nichols and D. S. Rimai (private communication).

ture<sup>3</sup>;  $\gamma_{th} = \alpha_v B / C_p$ , where  $\alpha_v = dV/VdT$  and  $C_p$  is the heat capacity per unit volume at constant pressure, and we use room-temperature values for  $B$ ,  $C_l$ , and  $(\partial C_l / \partial P)_T$  inside the brackets. (Table II contains values for various quantities used in calculating  $\Delta C_l / C_l$ .) From these calculations we found  $\Delta C_l / C_l = -0.088$  for *a*-As<sub>2</sub>S<sub>3</sub> and  $-0.082$  for *a*-As<sub>2</sub>Se<sub>3</sub>, whereas experimental values of  $2\Delta v_l / v_l + 3\Delta L / L$  are  $-0.096$  for *a*-As<sub>2</sub>S<sub>3</sub> and  $-0.097$  for *a*-As<sub>2</sub>Se<sub>3</sub>. The closeness of the calculated values to the experimental ones suggests that Eq. (1) will be able to account for our  $v_l$ -vs- $T$  results, since our use of the room-temperature value of  $\gamma_{th}$  for  $\gamma$  is expected to yield an underestimate of  $-\Delta C_l / C_l$  because  $\gamma_{th}$  increases considerably with decreasing temperature.<sup>3</sup> Such behavior of  $\gamma_{th}$  can be understood in terms of the deexcitation of higher-frequency modes possessing smaller  $\gamma_i$ 's as the temperature falls, since  $\gamma_{th} = \sum C_{vi} \gamma_i / \sum C_{vi}$ , where  $C_{vi}$  is the heat capacity of mode  $i$ . Evidence that there may be small  $\gamma_i$  modes in *a*-As<sub>2</sub>S<sub>3</sub> is provided by Raman studies on crystalline As<sub>2</sub>S<sub>3</sub>.<sup>19</sup>

Next we investigate the temperature dependence of longitudinal-wave velocity implied by Eqs. (1) and (2) in more detail, and compare it with that observed. Using those equations, we have

$$v_l = v_l(1.5 \text{ K})(L/L_0)^{3/2} [1 - \Gamma_l F(T/\Theta)]^{1/2}, \quad (4)$$

where  $F(T/\Theta)$  is the bracketed quantity in Eq. (2).  $\Gamma_l$  depends on the coefficient of  $U$  in Eq. (1), of course. Assuming that it is a constant of the material, i.e., it is independent of temperature, and requiring Eq. (4) to fit the velocities measured at 1.5 and 296 K, we obtain  $\Gamma_l = 0.061$  for *a*-As<sub>2</sub>S<sub>3</sub> and  $\Gamma_l = 0.053$  for *a*-As<sub>2</sub>Se<sub>3</sub>. Using these values of  $\Gamma_l$

in Eq. (4), we then calculated the velocity versus temperature curves shown in Figs. 1 and 3. From these figures it can be seen that the calculated curves approximate the experimental data well above about 250 K, but rise above the data points for lower temperatures before rejoining the latter again at lowest temperatures. The most likely reason for the discrepancies down to perhaps 40 K is the temperature dependence of  $\Gamma_l$ . The  $T$  dependence of  $C_l/3B$  is negligible, so that if  $(\partial C_l / \partial P)_T$  is almost independent of temperature, as is usually the case in solids and is implied for our glasses by velocity versus pressure measurements<sup>20</sup> on *a*-As<sub>2</sub>S<sub>3</sub> and *a*-As<sub>2</sub>Se<sub>3</sub> at 195 and 296 K, then the variation of  $\Gamma_l$  with temperature would be due to the temperature dependence of  $\gamma$ . We found the values of  $\gamma$  needed at various temperatures to make Eq. (1) fit our velocity data on *a*-As<sub>2</sub>S<sub>3</sub> and *a*-As<sub>2</sub>Se<sub>3</sub> down to 40 K. We show these  $\gamma$  values in Fig. 9, and for the sake of clarity, will henceforth refer to them as  $\gamma_{us}$  values. The reasonableness of the  $\gamma_{us}$  values becomes apparent when we compare them with the thermodynamic  $\gamma$  versus temperature results<sup>3</sup> shown in Fig. 9, and with the low-temperature elastic  $\gamma$ 's (which will be discussed in Sec. IV B).

The  $\gamma_{us}$  values obtained above from our longitudinal-velocity data will now be used in interpreting our shear-velocity versus temperature data. Adapting the results of GG, we find for  $C_t$  the elastic stiffness modulus of transverse waves:

$$C_t = C_t^0 + \frac{1}{V} \left\{ -\gamma^2 (U + C_v T) - \gamma \left[ \left( \frac{\partial C_t}{\partial P} \right)_T - \frac{C_t}{3B} \right] U \right\}, \quad (5)$$

where  $C_v = dU/dT$  is the heat capacity at constant volume. Inserting  $\gamma_{us}$  for  $\gamma$ ,  $U + C_v T$  from the De-

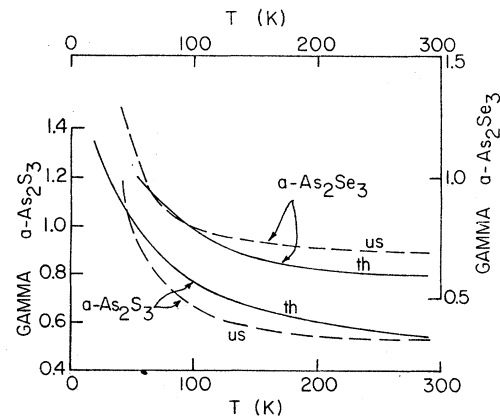


FIG. 9. Thermodynamic Grüneisen  $\gamma$  from Ref. 3 (solid curve) and ultrasonic  $\gamma$  determined in this work (dashed curve).

bye model, and experimental values for the other quantities and the thermal expansivity, we calculated values of  $v_t$  as a function of temperature between 40 and 296 K. They agree very well with the measured velocities as can be seen in Figs. 2 and 4.

Thus we have shown that the temperature dependences of the elastic stiffness moduli in  $\alpha$ - $As_2S_3$  and  $\alpha$ - $As_2Se_3$  between 40 and 296 K can be understood very well in terms of the anharmonicity of vibrational modes describable by a Debye model. It is not clear if this explanation of velocity versus temperature data in our materials, which have pyramidal bonding, will be useful for interpreting velocity data on tetrahedrally bonded glasses. This is because in the latter, which include  $SiO_2$ ,  $GeO_2$ , and  $BeF_2$  glasses, the velocity has a different type of temperature dependence in the same temperature range, i.e., the velocity goes through a minimum.<sup>12</sup> For vitreous  $SiO_2$  this behavior might be explained partly by the fact that the elastic stiffnesses are decreased by pressure and the thermal-expansion coefficient is positive above 175 K but negative at lower temperatures. In addition, the velocity minimum in vitreous  $SiO_2$  is influenced by the large attenuation maximum which occurs at moderately low temperatures in this material.<sup>1,14</sup>

#### B. Temperature dependence of the velocity at lowest temperatures

The ultrasonic velocities in our samples begin to show measurable decreases with increasing temperature even at the lowest temperatures we employed, whereas the QH Debye solid is expected to exhibit measurable decreases only at higher temperatures. This can be seen in Figs. 5–8, which display both our data and dashed curves calculated for the QH Debye solid from Eqs. (1) and (5), using for  $\gamma$  a value deduced from room-temperature elastic  $\gamma's$ <sup>21</sup> combined in a manner appropriate for lowest temperatures. Specifically,

$$\gamma_{LT}^{elast} = [(v_t/v_l)^3 \gamma_t + 2\gamma_l] / [2 + (v_t/v_l)^3], \quad (6)$$

where the elastic  $\gamma's$   $\gamma_l$  and  $\gamma_t$  are given by

$$\gamma_j = -\frac{\partial \ln \omega_j}{\partial \ln V} = -\frac{1}{6} + \frac{1}{2} \frac{B}{C_j} \frac{\Delta C_j}{\Delta P} \quad (7)$$

with  $j=l$  and  $t$  for longitudinal and transverse (shear) waves, respectively. It is appropriate to use  $\gamma_{LT}^{elast}$  for  $\gamma$  in Eqs. (1) and (5) because only the lowest-lying vibrational modes are excited at low temperatures, and they are acoustical modes. Furthermore the values of  $\gamma_{LT}^{elast}$  (1.80 for  $\alpha$ - $As_2S_3$  and 1.84 for  $\alpha$ - $As_2Se_3$ ) are reasonable extrapolations

of the values we deduced above for  $\gamma_{us}$ . It should be noted that our  $-\Delta v/v$  data have different temperature dependences than the dashed curves, but do approach the latter near the upper end of the  $T$  range, as they should, to be consistent with results in Sec. IV A. If we had required Eq. (1) to fit our velocity data at lowest temperatures, very large, temperature-dependent  $\gamma's$  would have been obtained. For example, for longitudinal waves in  $\alpha$ - $As_2S_3$   $\gamma_{us}$  would have to be about 13 at 11 K and higher at lower  $T$ .

Since we have no reason to think that such large  $\gamma's$  are associated with the anharmonicity of vibrational modes, we think that the behavior we observe for  $\Delta v/v$  at lowest temperatures is due to relaxation processes involving tunneling in two-level systems. Such an explanation has been successful in accounting for a similar type of decrease in  $v$  with increasing  $T$  between about 1.5 and 3.5 K in silica glasses.<sup>1,9</sup> (Although resonant tunneling<sup>1</sup> has been found to be responsible for some ultrasonic effects in silica glasses, it can be ruled out as a cause of our results since it is characterized by an increase in velocity<sup>9</sup> with increasing  $T$ , which occurs in a lower temperature range—0.3 to about 1.0 K.) The relaxation processes are a consequence of the separations between the two energy levels in two-level systems being changed by the ultrasonic wave—presumably via deformation-potential coupling. The relative change of occupancy of the levels called for by the change in energy separations lags the ultrasonic strain, and involves tunneling of entities from one level to the other of a pair with the assistance of thermal phonons.<sup>10</sup> Such an origin for the  $T$  dependence of the velocities in our samples at low  $T$  is supported by the fact that the ultrasonic attenuation in  $\alpha$ - $As_2S_3$ ,<sup>2</sup> and  $\alpha$ - $As_2Se_3$ ,<sup>4</sup> can be interpreted using the DPW version of the two-level-systems model.

A rigorous interpretation of our  $\Delta v/v$ -vs- $T$  data at low temperature in terms of the tunneling model would require taking into account<sup>9</sup> the numbers of two-level systems having various energy differences  $\epsilon$ , tunneling energies  $\Delta$ , and the correlation between  $\epsilon$  and  $\Delta$ ;  $\epsilon$  is the difference between the two energy levels of a two-level system in the absence of tunneling and  $\Delta = \hbar \omega_0 e^{-\lambda}$ , where in the DPW model  $\omega_0$  is an atomic vibrational frequency and  $\lambda$  is the tunneling parameter given by  $d(2mV_b)^{1/2}/2\hbar$ . (In the latter,  $d$  is the separation and  $V_b$  the potential barrier between adjacent sites and  $m$  is the mass of the tunneling entity.) Doing this properly would require more information than is

### III. CALCULATION AND RESULTS

The phonon frequency shift  $\Delta_k(\omega)$  and width  $\Gamma_k(\omega)$

available from experiment, at least up to now. Therefore we shall use an expression<sup>1</sup> which involves some simplifications including the assumption that the products of deformation potentials with  $\epsilon/E$  or  $\Delta/E$ , where  $E=(\Delta^2+\epsilon^2)^{1/2}$ , are constant. The expression is

$$\frac{\Delta v_j}{v_j} = -\frac{M_j'^2}{2\rho v_j^2 kT} \int \frac{P(E) \operatorname{sech}^2(E/2kT) dE}{1+\omega_j^2 \tau^2}, \quad (8)$$

where  $j$  stands for longitudinal or transverse ultrasonic waves with (angular) frequency  $\omega_j$ , and  $M_j'=(\epsilon/E)D_j$ . For single-thermal-phonon-assisted tunneling,

$$\tau = \left( \frac{M_l^2}{v_l^5} + \frac{2M_t^2}{v_t^5} \right)^{-1} \frac{2\pi \rho \hbar^4}{E^2} \tanh(E/2kT), \quad (9)$$

where  $M_j=(\Delta/E)D_j$ . The  $D_j$  are deformation potentials. A value for the weighted average of  $M_l$  and  $M_t$  can be obtained from very-low-temperature thermal conductivity  $K$  and specific-heat data. Since  $K=\frac{1}{3}\sum C_{v_i} v_i^2 \tau_i$ , one obtains<sup>22</sup>

$$\bar{M}_K^2 = (v_l + \frac{1}{2}v_t)(v_l/M_l^2 + v_t/2M_t^2)^{-1}.$$

For  $a\text{-As}_2\text{S}_3$ ,  $\bar{M}_K=0.060$  eV. From Eq. (8), we have

$$M_l'^2/M_t'^2 = (v_l/v_t)^2 (\Delta v_l/v_l) / (\Delta v_t/v_t).$$

Using our experimental data in this relation, we find  $M_l'^2 \approx 1.7M_t'^2$  for both  $a\text{-As}_2\text{S}_3$  and  $a\text{-As}_2\text{Se}_3$ . This result has implications for how  $M_l$  is related to  $M_t$  and  $D_l$  is related to  $D_t$ , since from their definitions  $M_l^2/M_t^2 = D_l^2/D_t^2 = M_l'^2/M_t'^2$ .

In Eq. (8),  $P(E)$  is the number of two-level systems per unit energy per unit volume. Since the experimental heat capacity<sup>8</sup> at very low  $T$  has both a larger  $T^3$  term than calculable from the Debye model using the elastic  $\Theta$  and a term linear in  $T$ , it has been inferred that

$$P(E) = n_0(1 + \eta E^2), \quad (10)$$

where  $n_0$  is the number of states per unit energy per unit volume when  $E=0$ . This form for  $P(E)$  allows the excess heat capacity below 0.7 K and  $\Delta v/v$  between 1.5 and 7 K to be calculated correctly. However, greatly different values of  $\eta$  are needed to account for  $C_v$  data ( $3.6 \times 10^7$  eV<sup>-2</sup>) and  $\Delta v/v$  data ( $8.5 \times 10^6$  eV<sup>-2</sup>) on  $a\text{-As}_2\text{S}_3$ . In addition, in order for calculations to fit the  $\Delta v/v$  data up to 7 K,  $P(E)$  must vanish at energies greater than about  $2 \times 10^{-3}$  eV (see Fig. 5).

Because of these inadequacies of Eq. (10), we sought and found a physically reasonable distribution which could account for both  $C_v$  and  $\Delta v/v$  data below 7 K. It is the Gaussian

$$P(E) = [N/\sigma(2\pi)^{1/2}] \exp[-(E-E_0)^2/2\sigma^2], \quad (11)$$

with  $N=6.5 \times 10^{19}$  cm<sup>-3</sup>,  $E_0=1.6 \times 10^{-3}$  eV, and  $\sigma=6.6 \times 10^{-4}$  eV. The success of a Gaussian in fitting our  $\Delta v/v$  data is not too surprising perhaps, since ultrasonic attenuation in  $a\text{-As}_2\text{S}_3$  has been fitted using a distribution composed of the product of two Gaussians,<sup>2</sup> one of which was a function of  $\epsilon$  and the other a function of the tunneling parameter  $\lambda$ . Values for parameters in the product-of-Gaussians distribution were chosen to fit attenuation data up to much higher temperatures (50 K) than we have chosen to fit our  $\Delta v/v$  data herein. That attenuation fit required considerably larger values for deformation potentials than are deduced from our present fits of  $\Delta v/v$  data. The reason we attempt to fit our  $\Delta v/v$  data, by means of Eq. (8), (9), and (11), only below 7 K is because some features are present in the attenuation that suggest that only at such temperatures is the simplest thermal-phonon-assisted tunneling likely to be the predominant relaxation process. At higher temperatures, multiple-phonon effects and tunneling via activation to an intermediate state may occur.<sup>4,23</sup> (The suggestive features in the attenuation<sup>4</sup> are a slight shoulder in the attenuation-versus- $T$  plots for  $a\text{-As}_2\text{S}_3$  and  $a\text{-As}_2\text{Se}_3$  between 3 and 10 K and a very small attenuation maximum in  $a\text{-As}_2\text{Se}_3$  whose location shifts between about 16 and 35 K for frequencies between 30 and 270 MHz, respectively. This maximum was interpreted as evidence for tunneling via an intermediate state.<sup>4</sup>)

Using Eqs. (8), (9), and (11), we calculated curves to fit our  $\Delta v/v$  data below 7 K, as shown in Figs. 5–8. The fits required  $M_l'=0.060$  eV,  $M_t'=0.045$  eV,  $M_l=0.060$  eV, and  $M_t=0.053$  eV. These values are about  $\frac{1}{5}$  of those found for silica-based glasses by others.<sup>1</sup> The values of  $E_0$  and  $\sigma$  that we found are reasonable in view of the maximum tunneling energy of  $2 \times 10^{-3}$  eV calculated from  $k\Theta e^{-\lambda}$  using the minimum value of  $\lambda$  permitted by tunneling theory.<sup>5</sup>

The absence of a significant dependence of  $\Delta v/v$  on frequency in  $a\text{-As}_2\text{S}_3$  and  $a\text{-As}_2\text{Se}_3$  is unlike the behavior found for borosilicate glass.<sup>1</sup> In view of Eqs. (8) and (9), this could be attributed to the arsenic sulfide and selenide glasses having smaller deformation potentials and/or values of  $\omega_j \tau$ , at energies of importance, than does borosilicate glass. The distributions given by Eqs. (10) and (11), with the parameter values needed to fit our  $\Delta v/v$  data, are consistent in that each yields about the same total concentration of states  $N_T$  for  $a\text{-As}_2\text{S}_3$  ( $6 \times 10^{19}$  cm<sup>-3</sup>). For comparison we note that specific-heat data<sup>8</sup> below 0.7 K have been utilized to obtain an  $N_T$  as high as  $3 \times 10^{19}$  cm<sup>-3</sup> and as low as  $3 \times 10^{16}$  cm<sup>-3</sup>. Ambiguity arises in obtaining a value of  $N_T$  from the specific heat,

since this property is sensitive only to excitations having a limited range of energies around  $kT$ .

If the  $6 \times 10^{19}$ - $cm^{-3}$  concentration of states does represent tunneling sulfur atoms in  $a-As_2S_3$ , as seems likely, then one out of every 400 sulfur atoms are tunnelers and the average distance between tunneling pairs is about 25 Å. Such values for the numbers and separations of tunneling pairs are quite reasonable in terms of the interpretation<sup>1</sup> of results on  $SiO_2$  glass.

However, similarity between the concentration of states in  $a-As_2S_3$  and in vitreous  $SiO_2$  may have less significance than has been believed in the past because the most important defect in arsenic sulfide and selenide glasses may not occur in  $SiO_2$ . This defect is a valence-alternation pair<sup>24</sup> comprised of one threefold coordinated and one singly coordinated chalcogen. Densities of these pairs, estimated<sup>24</sup> from the theory or inferred from experiment ( $10^{17}$ - $10^{19}$   $cm^{-3}$ ), are not unlike the value we deduced above for  $N_T$  from our ultrasonic velocity data. Therefore we wonder if the two-level systems in  $a-As_2S_3$  (and  $a-As_2Se_3$ ) are valence-alternation pairs, and if movement of bond charge (electronic tunneling) causes the affects attributed to transition with two-level systems and ionic tunneling. Definitive experimental evidence for a bond-motion interpretation of ultrasonic effects has not been found, as far as we know. We have performed some ultrasonic attenuation experiments on  $a-As_2S_3$  utilizing magnetic or electric fields to check for electronic effects. They will be discussed elsewhere. Suffice it to say here that the applied magnetic fields did not influence the attenuation to within the experimental accuracy,<sup>4</sup> but that high electric fields produced some after effects<sup>25</sup> whose nature is still to be determined.

Before ending this section, we should point out that although in our analysis we have assumed that ultrasonic measurements "see" the same two-level systems which cause the excess heat capacity, this may not be true, because the coupling to ultra-

sonic strain (and the deformation-potential factors) could be energy dependent. This would explain the apparent discrepancies between the distributions sometimes inferred from heat-capacity and ultrasonic data. If fewer two-level systems contribute to ultrasonic effects than to the heat capacity, then larger values for the  $M_i''$ 's, and presumably the deformation potentials, would be needed to fit our  $\Delta v/v$  data.

## V. CONCLUSION

The ultrasonic velocity in  $As_2S_3$  and  $As_2Se_3$  glasses was found to be independent of frequency, indicating that the dispersion reported previously<sup>2</sup> in  $a-As_2S_3$  was erroneous (probably because of improper overlapping of echoes).

The temperature dependence of the velocities in  $a-As_2S_3$  and  $a-As_2Se_3$  is explainable by means of the QH Debye model from 296 down to 40 K and in terms of relaxation processes involving thermal-phonon-assisted tunneling in two-level systems at lower temperatures.

Theoretical expressions for the QH Debye solid can be fitted to our data above 40 K and for single-phonon-assisted-tunneling relaxation processes to our data below 7 K, yielding, respectively, reasonable values for a  $T$ -dependent ultrasonic  $\gamma$  and for the distribution of energy separations and deformation potentials of two-level systems.

The adequacy of the QH Debye model for our higher- $T$  data seems to rule out a significant temperature dependence in the velocity due to the processes which cause the attenuation<sup>2,3</sup> at ordinary  $T$  to be much larger than it is in crystalline dielectric solids.

## ACKNOWLEDGMENTS

We wish to express our gratitude to M. Kariya of the Nikon Co. and P-W. Li of the 3-M Co. for  $a-As_2Se_3$  samples, and to D. Ng and J. G. Bennett for experimental advise and assistance. Support was provided by NSF Grant Nos. DMR-72-03012A2, DMR-72-03018A03, and DMR-77-08476.

\*Present address: Argonne National Laboratory, Argonne, Ill. 60439.

<sup>1</sup>S. Hunklinger and W. Arnold, in *Physical Acoustics*, edited by R. N. Thurston and W. P. Mason (Academic, New York, 1976), Vol. 12, p. 155.

<sup>2</sup>D. Ng and R. J. Sladek, *Phys. Rev. B* **11**, 4017 (1975).

<sup>3</sup>T. N. Claytor and R. J. Sladek, in Proceedings of the Sixth International Conference on Amorphous and Liquid Semiconductors, Leningrad, USSR, 1975 *Structure and Properties of Non-Crystalline Semiconductors*, edited by B. T. Kolomiets (Academy of

Sciences of USSR, A. F. Ioffe Physical-Technical Institute, 1976), p. 54.

<sup>4</sup>T. N. Claytor, Ph.D. thesis (Purdue University, 1976) (unpublished).

<sup>5</sup>P. W. Anderson, B. I. Halperin, and C. M. Varma, *Philos. Mag.* **25**, 1 (1972).

<sup>6</sup>W. A. Phillips, *J. Low Temp. Phys.* **7**, 351 (1972).

<sup>7</sup>R. C. Zeller and R. O. Pohl, *Phys. Rev. B* **4**, 2029 (1971).

<sup>8</sup>R. B. Stephens, *Phys. Rev. B* **8**, 2896 (1973).

<sup>9</sup>L. Piché, R. Maynard, S. Hunklinger, and J. Jäckle,



- Phys. Rev. Lett. 32, 1426 (1974).
- <sup>10</sup>J. Jäckle, Z. Phys. 257, 212 (1972).
- <sup>11</sup>J. T. Krause and C. R. Kurkjian, J. Am. Ceram. Soc. 51, 226 (1968).
- <sup>12</sup>J. T. Krause, Phys. Lett. 43, 325 (1973).
- <sup>13</sup>O. L. Anderson and H. E. Bömmel, J. Am. Ceram. Soc. 38, 125 (1955).
- <sup>14</sup>C. K. Jones, P. G. Klemens, and J. A. Rayne, Phys. Lett. 8, 31 (1964).
- <sup>15</sup>E. P. Papadakis, J. Acoust. Soc. Am. 42, 1045 (1967).
- <sup>16</sup>M. Hortal, Phys. Chem. Glasses 19, 5 (1978).
- <sup>17</sup>G. Leibfried and W. Ludwig, in *Solid State Physics*, edited by F. Seitz and D. Turnbull (Academic, New York, 1956), Vol. 2, p. 276.
- <sup>18</sup>J. A. Garber and A. V. Granato, Phys. Rev. B 11, 3990 (1975).
- <sup>19</sup>R. Zallen, Phys. Rev. B 9, 4485 (1974).
- <sup>20</sup>D. Nichols and D. S. Rimai (private communication).
- <sup>21</sup>C. S. Smith, D. E. Schuele, and W. B. Daniels, in *Physics of Solids at High Pressures*, edited by C. Tomizuka and R. Emrick (Academic, New York, 1965), p. 496.
- <sup>22</sup>M. P. Zaitlin and A. C. Anderson, Phys. Rev. B 12, 4475 (1975).
- <sup>23</sup>J. A. Sussman, Phys. Kondens. Mater. 2, 146 (1964).
- <sup>24</sup>M. Kastner, D. Adler, and H. Fritzsche, Phys. Rev. Lett. 37, 1504 (1976).
- <sup>25</sup>T. N. Claytor (private communication).